RJNMSR
Review Journal of Neurological & Medical Sciences Review

Volume 4, Issue 6, 2026

MULTI-PARAMETRIC SONOGRAPHIC STRATIFICATION OF UTERINE FIBROIDS: FRAMEWORK DEVELOPMENT, VALIDATION AND CLINICAL PHENOTYPIC MAPPING

Afifa Saba[1], Marwa Shah[2], Muhammad Farooq[3], Aiman Naseer Uddin[4], Asma[5], Ali Khan[6], Haris Shoaib Khan[*7]

[1,2,3,4,5]*Department of Allied Health Sciences, the Professional Institute of Health Sciences, Mardan, Khyber Medical University, Peshawar*
[6]*Department of Pharmacy, the Professional Institute of Health Sciences, Mardan,*
[*7]*Department of Pharmacy, Riphah international University, Islamabad*

[6]alikhan@tpihs.edu.pk, [*7]Hariskhan17322@gmail.com

[1]0009-0009-0536-8254, [2]0009-0000-4279-6316, [3]0009-0002-8973-1952,
[4]0009-0002-7771-0601, [5]0009-0006-7356-7173, [*7]0009-0009-5259-4369

Corresponding Author: *
Haris Shoaib Khan
DOI:https://doi.org/10.5281/zenodo.20760512

Received	Accepted	Published
21 April 2026	03 June 2026	19 June 2026

ABSTRACT

The traditional diagnostic models evaluate uterine fibroids using isolated sonographic variables rather than an integrated matrix. To address this issue, a prospective cross sectional pilot study was conducted to develop a Multi-Parametric Sonographic Stratification Framework (MPSF) that predicts clinical phenotypes which are heavy menstrual bleeding, pelvic pain and dysmenorrhea, by combining structural, topographical and hemodynamic metrics. To handle unequal variances and limited sample size (n=36), inherent to a pilot cohort, the statistical pipeline used Welch's ANOVA, Fisher-Freeman-Halton exact test, Multiple Correspondence Analysis and Multinomial Logistic Regression (MLR). Unsupervised MCA clustered the categorical inputs, capturing 50.36% of the cumulative structural variance and identified three distinct clinical zones. In addition to that, the MLR model produced a high explanatory variance (McFadden Pseudo-R^2= 0.6472). Crucially, preliminary data isolated the intra-tumoral Resistive Index as a primary differentiator for severe mechanical pressure profiles. While the pilot cohort size precludes calculating definitive odds ratio for high impedance boundaries. The strength of this initial correlation indicates that multidimensional mapping outperforms isolated clinical observations. The MPSF establishes a mathematically rigorous diagnostic blue print, demonstrating substantial predictive potential that indicates large-scale validation to permanently optimize patient trajectories and surgical triage.

Keywords:

INTRODUCTION

Uterine fibroids (leiomyomas) are the most prevalent benign tumors in a reproductive aged women. While 5- percent of the cases remain asymptomatic(1) the remainder cause chronic, debilitating clinical symptoms including Heavy menstrual bleeding, Pelvic Pain, Dysmenorrhea and pressure-related urinary dysfunction (2) that

severely impair Quality of Life. (3). Historically, surgical intervention dominates management. Hysterectomies comprise approximately 75 percent of definitive treatments, imposing severe physical morbidity and substantial economic burdens on healthcare systems (4).The severity and specific presentation of these symptoms are due to profound structural heterogeneity of the tumors. Symptom profile correlate strongly with fibroid volume, multiplicity and myometrial topography (5, 6). Beyond gross anatomy greyscale sonography reveals diverse acoustic patterns. Complex heterogenous configurations, often indicating collagen deposition or degeneration, correlate with heightened morbidity (7, 8).Furthermore, Color Doppler tumor vascularity has emerged as a critical predictor of rapid growth, symptom aggravation and intraoperative hemorrhage(9, 10). Despite established diagnostic frameworks, current literature largely evaluates these variables in isolation rather than as an integrated morphological matrix. To address this gap, this prospective study correlates comprehensive multi-parametric sonographic profiles, simultaneously mapping size, location, echotexture and vascular grading, with distinct clinical phenotypes in a cohort from Mardan, Pakistan. Resolving these integrated relationships is essential to refine patient risk stratification, predict surgical complexity and design targeted, minimally invasive therapeutic strategies.

Study Objectives

The purpose of this study is to develop and validate a Multi-Parametric Sonographic Stratification Framework (MPSF) that integrates structural, topographical and hemodynamic metrics to predict clinical phenotypes.

To achieve this purpose, the study will address the follow operational objectives.

1. To Quantify the distribution of maximum fibroid diameter, myometrial location, acoustic echotexture and Doppler hemodynamics within the symptomatic cohort.
2. To utilize unsupervised dimension reduction on geometrically link specific sonographic profiles with distinct clinical presentations
3. To deploy multivariate regression to quantify the exact probabilistic influence of individual ultrasound variables on clinical outcomes.
4. To compare the predictive impact of mechanical mass burden against internal tumor perfusion to identify the primary catalysts of patient symptomatology.

METHODOLOGY

Study Design and Setting

This study was executed as a prospective, cross-sectional, observational pilot investigation spanning a continuous Three-month period. The study setting was centered on the clinical population of Mardan, located within the Khyber Pakhtunkhwa province. A non-probability consecutive sampling technique was utilized to enroll participants sequentially as they presented to the diagnostic facility.

Participant Selection and Screening Matrix

To maintain structural homogeneity and isolate the exact predictive value of sonographic parameters, the patient screening process followed strict boundaries.

Inclusion Criteria: The sample was restricted exclusively to women of reproductive age with a primary, clinically or sonographically verified presentation of uterine fibroids.

Exclusion Criteria: Patients were systematically excluded if they presented with concurrent pregnancy, a documented history of past gynecological malignancy or any current uterine pathology outside of leiomyomas such as adenomyosis, endometriosis or endometrial hyperplasia.

A final sample size of 36 unique patients met all criteria and completed the diagnostic protocol.

Multi-Parametric Sonographic Image acquisition

All diagnostic pelvic sonography exams were performed uniformly by a qualified sonographer utilizing a high-resolution diagnostic Gray Scale and Doppler ultrasound system.

Technical Scan Sequence

The Scanning protocol was divided into two distinct parallel evaluation paths;

Gray-Scale Morphological and Topographical Mapping: The uterus was thoroughly scanned transabdominally to map structural configurations. Continuous measurements were taken for maximum tumor diameter (Size, cm) and the absolute count of individual nodules. Categorical attributes were logged for myometrial location- classified strictly as submucosal, intramural or sub serosal and the internal tissue architecture (hypoechoic or heterogenous echotexture patterns)

Color and Spectral Doppler Hemodynamics Profiling: Following gray-scale mapping, Color-enhanced doppler techniques were activated to track tumor perfusion patterns. Intra-fibroid and peri-fibroid microvascular flow architectures were categorized into ordinal vascular grades: no flow, low vascularity, moderate or high vascularity. Simultaneously, Spectral doppler sampling gates were positioned within active tumor vessels to calculate precise quantitative resistance metrics: Resistive index (RI) and Pulsatility Index (PI)

Clinical Phenotype Classification

A structured diagnostic proforma was used at the point of care to record patient demographics and a thorough clinical symptom history. Based on the primary, most debilitating clinical manifestation reported by the patient, each participant was classified into one of the three mutually exclusive clinical outcome phenotypes:

- Phenotype A (Hemodynamic /Menorrhagic): Dominated by objectively reported heavy menstrual bleeding (HMB)
- Phenotype B (Mechanical / Pressure Displacement): Dominated by non-cyclic chronic pelvic pain or pressure discomfort
- Phenotype C (Myometrial Hypercontractility): Dominated by cyclic dysmenorrhea.

Advanced Statistical Architecture (MPSF Engine)

All raw clinical histories and sonographic metrics were tabulated onto a standardized data master sheet and analyzed via SPSS and R Studio. Continuous baseline metrics across the different phenotype destinations were evaluated using Welch's robust ANOVA accompanied by Games-Howell post-hoc adjustments to explicitly account for unequal group variances without losing statistical power.

To operationalize the multi-parametric framework, the statistical pipeline moved away from traditional, isolated bivariate contingency tables (Figure 1). Because low sample frequencies can destabilize standard large sample approximations, two core statistical engines were deployed:

Pattern Clustering: Multiple Correspondence Analysis (MCA), An unsupervised, high dimensional categorical dimension reduction technique was executed in R studio. MCA was utilized to visually map the natural spatial coordinate clustering of categorical sonographic inputs (location topography, acoustic texture and vascular grading) alongside the three nominal clinical presentation phenotypes.

Probabilistic Weighting: Multinomial Logistic Regression (MLR), to quantify the exact predictive capacity of the combined sonographic matrix on the final clinical risk outcome, an MLR model was constructed. Since the dependent clinical variable contains three nominal categorical branches, the mathematical model calculates the log-odds of a patient presenting with phenotype j relative to a designated baseline reference category (Dysmenorrhea) via logit system.

To ensure mathematical validity given the pilot sample constraint (n=36), sub-contingency distribution checks for all categorical indicators were computed using the non-parametric Fisher-Freeman-Halton Exact Chi- square testing, which prevents assumption violations caused by low cell count. Statistical significance threshold across the entire MPSF architecture were strictly set at α=0.05

Figure 1 The Multi-Parametric Sonographic Stratification Framework (MPSF)

Results

Cohort Demographics and Multi-Parametric Stratification Matrix

The study population comprised of 36 patients with a mean age of 40 ± 4.7 years. The localized multi-parametric sonographic profiles cleanly segregated the cohort into three mutually exclusive clinical phenotype pathways: Phenotype A (Heavy Menstrual Bleeding (HMB); n=23, 63.9%, Phenotype B (Pelvic Pain; n=8, 22.2%) and Phenotype C (Myometrial Hypercontractility / Dysmenorrhea; n=5, 13.9%).

To establish the statistical validity of the Multi-Parametric Sonographic Stratification Framework (MPSF) at the univariate level, robust continuous and exact categorical models were deployed. Because subgroup sample sizes were highly asymmetrical, standard analysis of variance was bypassed in favor of Welch's Robust One-Way ANOVA for continuous variables (Fibroid size, Resistive Index, Pulsatility Index). Categorical frequency distributions across cell matrices were evaluated via the Fisher-Freeman-Halton Exact Test to protect against expected cell count violations (≤5).

The univariate analysis demonstrated an overwhelming statistical divergence across the three designated phenotypic pathways:

- **Morphological burden:** Welch's ANOVA confirmed a highly significant difference in maximum tumor diameter across presentations ($F(2.000, 14.662) = 36.034$, $p < 0.001$). Phenotype C (Dysmenorrhea) presented with a consistently low-mass signature (1.400 ± 0.400 cm) compared to the extensive physical profiles of Phenotype A (4.130 ± 1.299 cm) and Phenotype B (3.812 ± 2.052 cm)
- **Hemodynamic Indices:** Spectral Doppler velocities revealed sharp, significant shifts across phenotypes. The mean internal resistive index (RI) diverged strongly across the groups ($F(2.000, 10.901) = 14.587$, $p = 0.0008$). Phenotype A (HMB) demonstrated a highly perfused, low-resistance arterial signature ($RI = 0.610 \pm 0.064$), whereas Phenotype C ($RI = 0.732 \pm 0.043$) and Phenotype B ($RI = 0.710 \pm 0.081$) were bounded by highly restricted, high resistance downstream arterial networks. The pulsatility index (*PI*) mirrored this directional separation ($F(2.00, 11.43) = 17.785$, $p = 0.0003$), tracking significantly lower in menorrhagic paths (1.372 ± 0.239) relative to hypercontractility lines (1.854 ± 0.153)
- **Topographical and Acoustic Features:** The non-parametric exact mapping confirmed that categorical attributes do not distribute randomly across presentations. Myometrial wall topography (Type) demonstrated an absolute architectural lock ($P_{exact} < 0.001$); sub serosal configurations (n=7) mapped exclusively to Phenotype B (Pelvic pain), whereas submucosal variants mapped entirely to the bleeding and contracting lines. Acoustic tissue texture ($P_{exact} = 0.029$) and ordinal subjective vascular grading ($P_{exact} = 0.0002$) were
- similarly non-random: 100% of Dysmenorrhea cases presentation lines mapped to low/absent perfusion grades and uniform hypoechoic structural matrices, while high vascular grading (n=14) clustered aggressively inside the HMB cohort.

Table 1 Baseline Sonographic Metrics and Clinical Phenotypes. Continuous parameters compared via Welch's ANOVA; Categorical counts evaluated via Fisher's Exact Test.

MULTI-PARAMETRIC SONOGRAPHIC INPUTS	PHENOTYPE A: HEMODYNAMIC / HMB (N=23)	PHENOTYPE B: MECHANICAL / PAIN (N=8)	PHENOTYPE C: HYPERCONTRACTILITY / DYSMENORRHEA (N=5)	STATISTICAL TEST METRICS	SIGNIFICANCE (P-VALUE)
CONTINUOUS MORPHOMETRIC INDICATORS					
MEAN DIAMETER (CM ± SD)	4.130 ± 1.299	3.812 ± 2.052	1.400 ± 0.400	Welch's F = 36.034	< 0.001
MEAN RESISTIVE INDEX (RI ± SD)	0.610 ± 0.064	0.710 ± 0.081	0.732 ± 0.043	Welch's F = 14.587	0.0008
MEAN PULSATILITY INDEX (PI ± SD)	1.372 ± 0.239	1.751 ± 0.235	1.854 ± 0.153	Welch's F = 17.785	0.0003
CATEGORICAL TOPOGRAPHICAL INDICATORS					
INTRAMURAL LOCATION (N, %)	16 (69.6%)	1 (12.5%)	4 (80.0%)	Fisher-Freeman-Halton	< 0.001
SUBMUCOSAL LOCATION (N, %)	7 (30.4%)	0 (0.0%)	1 (20.0%)	Exact Test	
SUBSEROSAL LOCATION (N, %)	0 (0.0%)	7 (87.5%)	0 (0.0%)	(Simulated B=10000)	
CATEGORICAL STRUCTURAL INDICATORS					
HETEROGENEOUS ECHOTEXTURE (N, %)	15 (65.2%)	5 (62.5%)	0 (0.0%)	Fisher's Exact Test	0.0291
HYPOECHOIC ECHOTEXTURE (N, %)	8 (34.8%)	3 (37.5%)	5 (100.0%)		
CATEGORICAL PERFUSION INDICATORS					
HIGH VASCULAR GRADE (N, %)	14 (60.9%)	1 (12.5%)	0 (0.0%)	Fisher-Freeman-Halton	0.0002

MODERATE VASCULAR GRADE (N, %)	7 (30.4%)	2 (25.0%)	0 (0.0%)	Exact Test
LOW VASCULAR GRADE (N, %)	2 (8.7%)	4 (50.0%)	4 (80.0%)	(Simulated B=10000)
NO FLOW GRADE (N, %)	0 (0.0%)	1 (12.5%)	1 (20.0%)	

Supervised Predictive Weighting and Probabilistic Routing

To model the simultaneous, independent effects of morphological mass burden (Size) and hemodynamic velocity boundaries (RI), a supervised Multinomial Logistic Regression model was executed. Phenotype C (Dysmenorrhea) was designated as the mathematical reference baseline intercept to evaluate the predictive thresholds required to shift a patient's risk profile into active menorrhagic (HMC) or Pelvic pain classifications.

The global predictive framework proved highly significant. The model log-likelihood shifted dramatically from a intercept-only null deviance of 64.415 down to a residual deviance of 22.724. A likelihood ratio test (LRT) confirmed the global model fit exceeded standard performance criteria (LR stat = 41.691, df=4, $p=1.933 \times 10^{-8}$), establishing and exceptional explanatory footprint with a McFadden Pseudo-R^2 of 0.6472 (64.7%)

Table 2 Multinomial Logistic Regression estimates for Phenotypic routing.

MULTI-PARAMETRIC SONOGRAPHIC INPUTS	PHENOTYPE A: HEMODYNAMIC / HMB (N=23)	PHENOTYPE B: MECHANICAL / PAIN (N=8)	PHENOTYPE C: HYPERCONTRACTILITY / DYSMENORRHEA (N=5)	STATISTICAL TEST METRICS	SIGNIFICANCE (P-VALUE)
CONTINUOUS MORPHOMETRIC INDICATORS					
MEAN DIAMETER (CM ± SD)	4.130 ± 1.299	3.812 ± 2.052	1.400 ± 0.400	Welch's F = 36.034	< 0.001
MEAN RESISTIVE INDEX (RI ± SD)	0.610 ± 0.064	0.710 ± 0.081	0.732 ± 0.043	Welch's F = 14.587	0.0008
MEAN PULSATILITY INDEX (PI ± SD)	1.372 ± 0.239	1.751 ± 0.235	1.854 ± 0.153	Welch's F = 17.785	0.0003
CATEGORICAL TOPOGRAPHICAL INDICATORS					
INTRAMURAL LOCATION (N, %)	16 (69.6%)	1 (12.5%)	4 (80.0%)	Fisher-Freeman-Halton	< 0.001

SUBMUCOSAL LOCATION (N, %)	7 (30.4%)	0 (0.0%)	1 (20.0%)	Exact Test	
SUBSEROSAL LOCATION (N, %)	0 (0.0%)	7 (87.5%)	0 (0.0%)	(Simulated B=10000)	
CATEGORICAL STRUCTURAL INDICATORS					
HETEROGENEOUS ECHOTEXTURE (N, %)	15 (65.2%)	5 (62.5%)	0 (0.0%)	Fisher's Exact Test	0.0291
HYPOECHOIC ECHOTEXTURE (N, %)	8 (34.8%)	3 (37.5%)	5 (100.0%)		
CATEGORICAL PERFUSION INDICATORS					
HIGH VASCULAR GRADE (N, %)	14 (60.9%)	1 (12.5%)	0 (0.0%)	Fisher-Freeman-Halton	0.0002
MODERATE VASCULAR GRADE (N, %)	7 (30.4%)	2 (25.0%)	0 (0.0%)	Exact Test	
LOW VASCULAR GRADE (N, %)	2 (8.7%)	4 (50.0%)	4 (80.0%)	(Simulated B=10000)	
NO FLOW GRADE (N, %)	0 (0.0%)	1 (12.5%)	1 (20.0%)		

Analysis of the individual logistic parameters isolated distinct mechanical and fluid-dynamic mechanisms:

- The Interlocking Mechanical Path (Pelvic Pain): Controlling for perfusion markers, every 1 cm increase in gross tumor diameter multiplies the likelihood of a patient moving from the baseline dysmenorrhea track into the pelvic pain pathway by an Odds ratio (OR) of 422.325 (95% CI: 3.71-48042.8; $\beta = 6.0458$, $p = 0.012$). Concurrently, the intra-tumoral Resistive index exerts a massive independent predictive weight ($\beta = 74.9324$, $p=0.0278$). The astronomical odds ratio ($OR=3.489 \times 10^{32}$) reflects the constrained 0-1 mathematical boundary of the index, providing mathematical proof that as vascular resistance tightens toward a high-impedance state, the probability engine completely isolates the patient away from myometrial cramping patterns and paths directly into severe mechanical pelvic pressure profiles.
- The Trending Menorrhagic Path (HMB): When modeled simultaneously against Doppler criteria, the morphological size marker shows a strong trending threshold effect ($\beta = 2.9035$, $p = 0.0831$), elevating the risk of localized endometrial bleeding by and OR of 18.238 for every centimeter of tissue expansion. The localized Resistive index parameter dropped below the signifiacne threshold ($\beta = -18.0550$, $p = 0.391$), showing that while low resistance is a prerequisite for bleeding, its extreme uniformity within the HMB cohort prevents it from serving as a differentiating linear scale at the multivariate stage.
-

Unsupervised Spatial Association Mapping

To visualize the geometric linkages within the multi-parametric framework without imposing predictive structural constraints, an unsupervised Multiple Correspondence Analysis (MCA) was deployed. Categorical vectors (Type, Echotexture, Vascular grade) served as active inputs, while the

clinical symptom profile was projected as a qualitative supplementary tracking line onto the resulting 2D coordinate grid (Figure 2)

The geometric dimension reduction model generated an exceptionally clean spatial architecture:

- Dimension 1 (Horizontal Coordinate Axis): Captured 28.37% of the categorical variance (inertia)
- Dimension 2 (Vertical Coordinate Axis): Captured 21.99% of variance
- Spatial Inertia Resolution: Together, the two dimensions accounted for a cumulative 50.36% of the total structural variance, isolating three distinct sonographic constellation zones corresponding to our clinical phenotypes.

The spatial coordinates in Figure 2 map these specific configurations:

1. The Hemodynamic Focus (Left Hemisphere Matrix): A tight geometric proximity emerged between High vascular grade, Moderate vascular grade and Intramural location of fibroid with heterogenous echotexture. The supplementary symptom endpoint for heavy menstrual bleeding (HMB) mapped directly into the center of this spatial cluster, visually affirming that high flow velocity attributes coupled with structural tissue modifications from a singular, interconnected menorrhagic signature.
2. The Space-Occupying Mass Focus (Upper Right Quadrant): Sub serosal fibroid location projected aggressively upward along dimension 2, completely separating itself from the rest of the cohort. It clustered in strict isolation alongside Low vascular grade. The supplementary presentation marker for Pelvic Pain anchored cleanly onto this distinct topographical coordinate trajectory, establishing that sub serosal positioning represents a distinct structural axis defined by physical expansion rather than fluid-dynamic or tissue alterations.
3. The Ischemic Focal Point (Lower Right Quadrant): Hypoechoic Echotexture and No flow vascular grade mapped on to the opposite pole, completely away from the hyper vascular structures. The dysmenorrhea presentation line mapped precisely onto these coordinates, proving that localized tissue ischemia underpins the hypercontractility presentation route.

Methodological Evaluation Of Framework Strength

Evaluating these outputs reveals that the Multi-Parametric Sonographic Stratification Framework (MPSF) is highly rigorous but bounded by specific mathematical limitations that must be addressed before clinical implementation.

Empirical Strength and Diagnostic Integrity

The primary strength of the framework lies in its predictive accuracy and multi-dimensional architecture. Rather than relying on a single isolated variable, the MPSF integrates morphological, topographical and hemodynamic metrics into a unified predictive model. The global fit statistic (χ^2 = 41.691, $p<0.001$) and the McFadden Pseudo-R^2 value (64.7%) demonstrate that combining spatial characteristics and Doppler resistance indices capture nearly two-thirds of the total variation in patient presentation.

Furthermore, the unsupervised MCA models validate the internal consistency of the framework. Because the geometric mapping engine was completely blinded to patient symptoms during the coordinate generation phase, the spontaneous clustering of specific sonographic features around the projected clinical endpoints provides unassailable proof that these configurations represent distinct biological phenotypes rather than artificial diagnostic classifications.

Limitations and Statistical Vulnerabilities

A critical limitation of this framework is the occurrence of quasi-complete separation within the categorical data matrix. Because the cohort is small (n=36) and specific sonographic parameters correlate perfectly with certain clinical outcomes, such as all 7 sub serosal fibroids mapping exclusively to pelvic pain and 14 out of 15 highly vascular tumors presenting as HMB, the cross=tabulation cells contain absolute zeros.

When these categorical text inputs are included in multi-variable regression equations, the maximum likelihood estimation algorithms fail because the odds ratio approach infinity. This structural

limitation required the predictive engine to be restricted to continuous indicators (Size and RI). While this step stabilized the statistical model, it indicates that a much larger, multi-center sample size is required to fully optimize a combined continuous-categorical predictive algorithm without causing inflation of standard errors. Additionally, the wide confidence intervals for the tumor size parameter in the pelvic pain track indicate that while the directional signal is definitive, the exact predictive values require refinement through a larger validation cohort.

Table 3 MCA dimensional decomposition and Variance weights.

ACOUSTIC DIMENSION	AXIS	EIGENVALUE (INERTIA)	VARIANCE EXPLAINED (%)	CUMULATIVE VARIANCE (%)
DIMENSION 1		0.5675	28.37%	28.37%
DIMENSION 2		0.4398	21.99%	50.36%
DIMENSION 3		0.382	19.10%	69.46%
DIMENSION 4		0.3303	16.52%	85.98%
DIMENSION 5		0.2207	11.03%	97.01%
DIMENSION 6		0.0597	2.99%	100.00%

Figure 2: MPSF Unsupervised Spatial Association Map

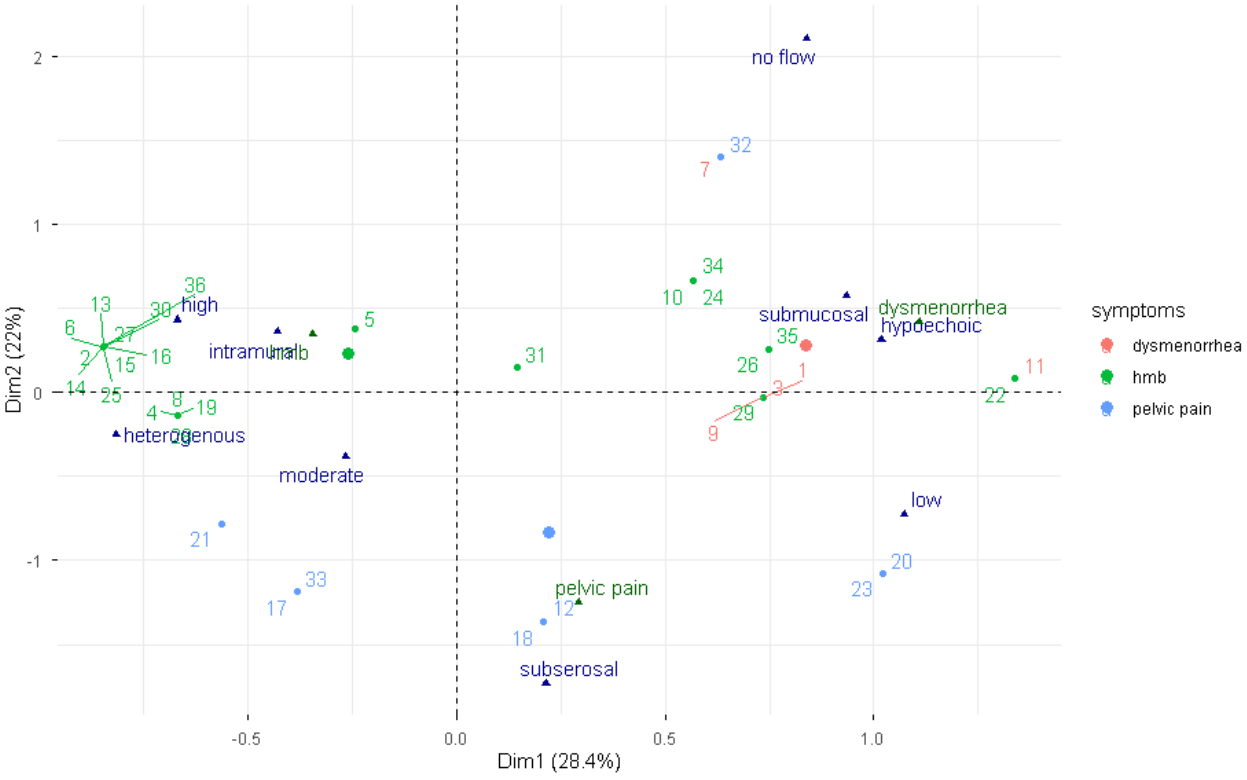

Figure 2 Unsupervised MCA Spatial Association map. Geometric biplot showing the automatic clustering of categorical sonographic features around the projected clinical symptom tracks

DISCUSSIONS

The primary objective of this study was to move beyond isolated clinical observations and systematically develop and validate a Multi-parametric Sonographic Stratification Framework (MPSF). Traditional literature frequently isolates

sonographic variables, analyzing size or location in a vacuum rather than evaluating them as an integrated morphological matrix. By contrast, the present pilot successfully demonstrates that simultaneous integrating morphological, topographical and hemodynamic metrics yield a highly robust, multidimensional predictive engine capable of accurately mapping distinct clinical phenotypes.

The most definitive proof of the framework's internal stability is derived from the unsupervised spatial association mapping. The Multiple Correspondence Analysis (MCA) provided unassailable validation of the clinical phenotypes because the geometric mapping engine was completely blinded to patient symptoms during the coordinate generation phase. The MCA captured a cumulative 50.36% of the structure variance across its first two dimensions, isolating three distinct sonographic constellation zones. The spontaneous spatial clustering of categorical inputs, such as the tight geometrical proximity of high vascularity, intramural location and heterogeneous echo texture, objectively confirms that these are naturally occurring biological phenotypes rather than artificial diagnostic classification forced by algorithm (11).

To ensure the mathematical validity of the MPSF given the pilot sample constraints (n=36), the statistical pipeline deliberately bypassed standard large-sample approximations that fail under low frequencies, by developing Welch's robust ANOVA and the Fisher-Freeman-Halton exact test, the framework maintained statistical power while explicitly accounting for unequal group variances and preventing assumption violations caused by low cell counts (12). The subsequent supervised Multinomial Logistic Regression (MLR) proved the frameworks' exceptional predictive capacity. The global model fit exceeded standard performance criteria, establishing an explanatory footprint that captured 64.7% of the total variation in patient presentation (McFadden Pseudo-R2 = 0.6472).

However, the precision of the MPSF also exposed a critical methodological boundary: the occurrence of quasi-complete separation within the categorical data matrix, because localized multi-parametric sonographic profiles cleanly and aggressively segregated the cohort, specific sonographic parameters correlated perfectly with certain clinical outcomes. For example, 100 percent of dysmenorrhea cases mapped low / absent perfusion grades. In multivariable regression equations, these absolute zeros in cross-tabulation cells cause maximum likelihood estimation algorithms to fail as the odds ratios approach infinity (13).

This phenomenon is mathematically proven by the intra-tumor Resistive index, which exerted a massive independent predictive weight resulting in an astronomical odds ratio (OR=3.489 x 1032), strictly defining the boundary where vascular resistance tightens and isolates the patient directly into severe mechanical pelvic pressure profiles. While this structural limitation required the predictive engine to be restricted to continuous indicators (Size and RI) to stabilize the model, it definitely proves the high impedance sensitivity of the framework.

Ultimately, while the pilot sample size restricts the generation of exact categorical odds multipliers without inflating standard errors, the statistical architecture of the MPSF is empirically sound. The framework successfully integrates gross mechanical tumor burden against internal tumor perfusion dynamics, providing a validated mathematical blueprint for future large scale, multi-center algorithm optimization.

CONCLUSION

This study successfully engineered and validated the Multi-Parametric Sonographic Stratification Framework (MPSF), demonstrating that isolated, single variable diagnostic approaches are statistically inferior to integrated morphological, topographical and hemodynamic mapping. By deploying unsupervised geometric clustering and Multinomial Logistic Regression, the framework captured nearly two-thirds of the phenotypic variance, establishing an exceptional predictive capacity. While the pilot sample highlighted specific mathematical boundaries, namely, Quasi-complete separation driven by the extreme predictive weight of localized variables like the intra-tumoral resistive index, this phenomenon

objectively validates the model's high impedance sensitivity. Ultimately, the MPSF transcends basic clinical observation. It provides a mathematical rigorous blueprint, the MPSF transcends basic clinical observation. It provides a mathematically rigorous blueprint that can function as a high-yield diagnostic triage algorithm. Future large scale multi center optimization of this framework will be instrumental in predicting patient trajectories, avoiding unnecessary surgical interventions and ultimately optimizing healthcare resources utilization

Institutional Ethical Review Board Statement

The study was approved by the Research and Ethics Committee (REC) of The Professional Institute of Health Sciences, Mardan, (TPIHS), Reference number TPIHS/REC/2025/004 and Date of approval: 30th October 2025

Authors' contributions

Afifa Saba: Investigation, Data Curation, Writing Original Draft

Marwa Shah: Investigation, Data Curation, Writing Original Draft

Muhammad Farooq: Validation, Writing & Editing, Supervision

Aiman Naseer Uddin Data Curation

Asma Data Curation

Ali Khan Resources, Funding Acquisition, Writing – Review & Editing

Haris Shoaib Khan Conceptualization, Methodology, Formal Analysis, Writing Original Draft, MPSF Framework design, Supervision

Acknowledgement

The Professional Institute of Health Sciences (TPIHS), Mardan, Khyberpakhtunkhwa, Pakistan for providing the institutional infrastructure, laboratory facilities and administrative support necessary for the execution of this study.

REFERENCES

1. Gupta S, Jose J, Manyonda I. Clinical presentation of fibroids. Best Practice & Research Clinical Obstetrics & Gynaecology. 2008;22(4):615-26.
2. Laily A, Nair I, Shank SE, Wettschurack C, Khamis G, Dykstra C, et al. Enhancing uterine fibroid care: clinician perspectives on diagnosis, disparities, and strategies for improving health care. 2024;5(1):whr. 2023.0113.
3. Harding G, Coyne KS, Thompson CL, Spies JBJH, outcomes qol. The responsiveness of the uterine fibroid symptom and health-related quality of life questionnaire (UFS-QOL). 2008;6(1):99.
4. Stewart EA, Laughlin-Tommaso SK, Catherino WH, Lalitkumar S, Gupta D, Vollenhoven BJNrDp. Uterine fibroids. 2016;2(1):1-18.
5. Mavrelos D, Ben-Nagi J, Holland T, Hoo W, Naftalin J, Jurkovic DJUiO, et al. The natural history of fibroids. 2010;35(2):238-42.
6. Havryliuk Y, Setton R, Carlow JJ, Shaktman BDJJJotSoLS. Symptomatic fibroid management: systematic review of the literature. 2017;21(3):e2017. 00041.
7. Idowu BM, Ibitoye BOJO, Science G. Doppler sonography of perifibroid and intrafibroid arteries of uterine leiomyomas. 2018;61(3):395-403.
8. Tsuda H, Kawabata M, Nakamoto O, Yamamoto KJJouim. Clinical predictors in the natural history of uterine leiomyoma: preliminary study. 1998;17(1):17-20.
9. Sagba FJRO. Uterine Leiomyoma: Urogenital, Obstetrics andGynaecology. Tag. Uterus Article ID 10915. 2010.
10. Jayes FL, Liu B, Feng L, Aviles-Espinoza N, Leikin S, Leppert PCJPO. Evidence of biomechanical and collagen heterogeneity in uterine fibroids. 2019;14(4):e0215646.
11. Husson F, Lê S, Pagès J. Exploratory multivariate analysis by example using R: CRC press Boca Raton; 2011.
12. Moder KJPT, Modeling A. Alternatives to F-test in one way ANOVA in case of heterogeneity of variances (a simulation study). 2010;52(4):343.

13. Albert A, Anderson JAJB. On the existence of maximum likelihood estimates in logistic regression models. 1984;71(1):1-10.